SPECIAL SECTION: SOFT CONDENSED MATTER

Laser-induced freezing in 2-d colloids

Chinmay Das, Pinaki Chaudhuri, A. K. Sood* and H. R. Krishnamurthy[†]

Department of Physics, Indian Institute of Science, Bangalore 560 012, India
[†]Also at Jawaharlal Nehru Centre for Advanced Scientific Research, Bangalore 560 064, India

Dielectric colloid particles prefer occupying the intensity maxima of an applied stationary interference pattern of laser beams. A 2-d system of colloidal liquid freezes to form a triangular lattice structure when the external laser modulation is in 1-d and the period of the intensity maxima is commensurate to that of the triangular lattice. In this article we review our recent simulation results on this phenomenon of laser-induced freezing.

1. Introduction

THE melting transition in 2-d systems is an extraordinarily interesting phenomenon. Long wave-length phonon modes are known to destroy the long range translational order in 2-d crystals. Nonetheless there is a sharp phase transition separating the low temperature 'crystalline' phase with power law decay of the translational order parameter correlations (quasi-long range order) from the high temperature 'liquid' phase with exponential decay of the order parameter correlations.

Topological defects (Box 1) are known to play an important role in this 'melting' process. The transition can be a two stage continuous transition through a hexatic phase as proposed by Kosterlitz, Thouless, Halperin, Nelson and Young (KTHNY)[1–3] (Box 2). Alternately, the crystal can directly melt through a first order transition to form the uniform liquid. One of the mechanisms proposed for such a first order transition is the spontaneous generation of grain-boundaries[4]. Experiments[5] and numerical simulations[6,7] suggest that a 2-d crystal can melt through either of the proposed mechanisms depending on the value of the core energy of the dislocations, which in turn depends on the microscopic interactions.

In the density wave picture of freezing[8], a liquid freezes to a crystalline structure when the free energy for spontaneously generated density waves corresponding to the crystalline structure becomes lower compared to that of the liquid. Consider an external field which couples to such density modulations. This will lower the free energy for structures having density modulation at the applied wave-vectors. If the externally applied field

has wave-vectors corresponding to a subset of the crystalline wave-vectors, it can induce a freezing transition because of the nonlinear coupling among the (density) order parameters.

In practice, generating such a modulating field corresponding to the particle separations in atomic systems is beyond our present experimental capabilities. Charge stabilized colloidal particles (polyballs), with the typical separation in the micrometre length scale and very high dielectric constant allow an easy implementation of the above experiment. In laser-induced freezing (LIF for short), one excites a subset of the crystalline density modulation modes by applying a stationary interference pattern of laser beams (obtained by superposing two laser beams). Because the separation scale of colloid particles is comparable to the optical wavelength, visible (laser) light can be used to produce such modulated structures. In this paper we discuss the LIF transition in colloids confined to 2-d, and in particular review our recent simulation results on LIF[9–12] which suggest a first-order transition for the system under consideration. Frey et al.[13] have recently extended the KTHNY dislocation mediated melting theory to LIF in 2-d. Our simulations suggest that an extension of the idea of grain-boundary induced melting may be needed to understand LIF in 2-d charge stabilized colloids.

The rest of this paper is organized as follows. In §2 we review the properties of the colloid particles which make them the ideal system for constructing optical matter and for studying 2-d melting. In §3 we review the phenomenon of laser-induced freezing. In §4 we present the phase diagram obtained from our Monte Carlo simulations. We discuss results from a Brownian dynamics study of the melting mechanism in §5. In §6, we present some very recent results from Monte Carlo simulations of LIF in hard sphere colloids which seem to show a reentrant melting unlike the charge stabilized colloids. Finally we conclude with some remarks about the studies that need to be undertaken for a complete understanding of laser-induced freezing.
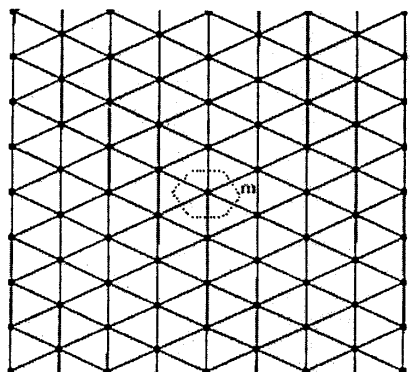
2. Charge stabilized colloids

Colloidal suspensions[14,15] are systems of particles dispersed in a solvent with particle sizes much larger than the atomic dimensions but small enough for the

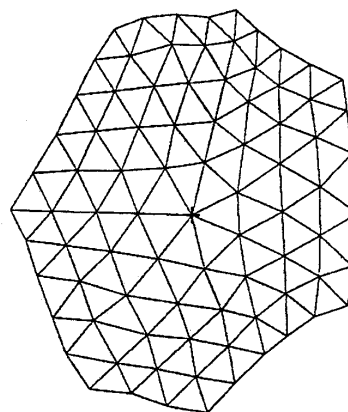---

*For correspondence. (e-mail: asood@physics.iisc.ernet.in)

Box 1. Defect structures in 2-d triangular lattices
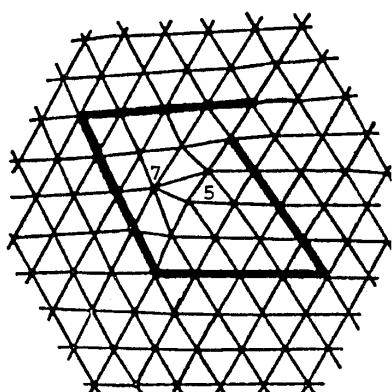
Triangular lattice

In a perfect triangular lattice, each of the particles has exactly six nearest neighbours. Nearest neighbours of particle *m* can be defined as the particles which participates in forming the Voronoi cell of the particle *m*. An ideal triangular lattice has both long-range translational and orientational order. The lines in the figure are to aid in identifying the neighbours.

Dislocation

Burgers circuit (denoted by the thick line) fails to close. The dislocation can be thought of as formed by two disclinations of opposite sign. A dislocation does not disrupt long-range orientational correlation, but badly affects translational order.
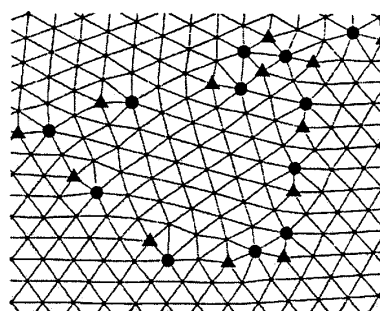
Disclination

A disclination for the triangular lattice is a particle which has number of nearest neighbours different from six. In the figure, the particle identified by + has seven nearest neighbours. Disclinations badly disrupt both orientational and translational order. (Figure adapted from ref. 34.)

Grain-boundaries

A grain-boundary is a separating line between two crystallites with different orientations and can be thought of as formed by a correlated string of dislocations (▲ and • refers to particles with five and seven neighbours, respectively.) The change of crystalline orientation, as one crosses a grain-boundary, depends on the Burgers vector of the grain-boundary. If the system is full of micro-crystallites, both the orientational and the translational orders are disrupted.

---

particles to be subjected to Brownian motion to prevent sedimentation due to gravity. The dynamics is governed by Langevin equations and there is a true thermodynamic temperature as opposed to the granular systems. The mechanism which prevents the particles from agglomeration can either be the presence of electric charges on the surface (called charge stabilization) or the adsorption or chemical binding of large molecules to the particles (called steric stabilization). Over the last few decades, the synthesis of spherical polymeric particles (polyballs) with a very narrow size distribution has

paved the way for studying the polyball systems as model condensed matter systems, with length and time scales suitable for performing many experiments which would be either beyond our capability or very difficult in the context of atomic systems. In this paper we mainly consider a model of aqueous suspension of mono-disperse charge stabilized polystyrene spheres. Each of these colloid particles is made of a large number of styrene polymeric chains entangled in a coil. These chains start and end with an acidic group, like $-KSO_4$. In a solvent with high dielectric constant, like

---

Box 2. KTHNY theory of melting

A dislocation pair, composed of two dislocations with opposite Burgers' vectors, cost an energy which is proportional to the logarithm of their separation[35]. So, at low temperatures, the dislocation pairs that are spontaneously generated are strongly bound and deform the lattice structure only locally, without affecting the global translational or orientational correlations. Kosterlitz and Thouless[1] predicted that a two-dimensional crystal melts at a temperature T_d by dissociation of these thermally generated dislocation pairs to form free dislocations which destroys the (quasi) long range translational order. Also according to their theory, the transition is continuous and is in the same universality class as XY model, 2d superfluids and 2d superconductors. From elasticity theory, the free energy cost for creating a dislocation pair with the smallest possible Burgers vector $|\vec{b}| = a$, the lattice vector, is given by:

$$\frac{F}{k_B T} = -K(T)\left[\ln\frac{R}{a_c} - \frac{1}{2}\cos^2(f)\right] + 2E_c . \tag{1}$$

Here the interaction coefficient $K(T)$ determined by the elastic moduli of the crystal, $R \equiv |\vec{R}|$ is the distance between the two cores of the dislocations with core sizes a_c and core energy E_c, and f is the angle between $\vec{b}$ and $\vec{R}$. Physically E_c is the energy associated with the destruction of the order parameter inside the dislocation core. The Kosterlitz-Thouless melting transition (KT) corresponds to the breakup of dislocation pairs with increasing temperature as the entropy term in the free energy connected with the large number of possible arrangements of the free dislocations becomes more important compared to the elastic energy cost.
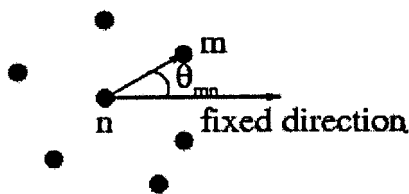
Halperin and Nelson[2] and independently Young[3] noted that the 2d particle systems have another relevant order parameter not addressed in the Kosterlitz–Thouless treatment. Define a local bond-orientational order parameter at the particle position r_n as

$$y_6(r_n) = \frac{1}{z_n}\sum_{m=1}^{z_n} e^{6iq_{mn}}, \tag{2}$$

where z_n is the number of nearest neighbours of the nth particle and q_{mn} is the angle of imaginary bond connecting nth particle with its mth neighbour about some fixed direction. $y_6(r)$ measures the local mean orientation modulo $p/3$ of all the nearest neighbours. Free dislocations destroy the (quasi) long range translational order but the orientational order remains (quasi) long-ranged. This liquid crystalline phase is called the hexatic phase and it has power law decay of the bond-orientational order parameter correlation function and exponential decay of the translational order parameter correlation function. Halperin, Nelson and Young considered the hexatic phase with the interaction free energy as,

$$\frac{F}{k_B T} = \frac{1}{2}K_A(T)\int d^2 r[\nabla q(r)]^2 , \tag{3}$$

where $q(r)$ is the phase of the bond-orientational order at r and stiffness constant K_A is called the Frank constant. Renormalization group technique gives another KT like transition at a temperature T_i ($> T_d$) to the isotropic liquid phase where both the bond-orientational and the translational order parameter correlations decay exponentially to zero. Physically a disclination is a particle having different co-ordination number as compared to the ideal lattice. A particle having more (less) number of nearest neighbours than the ideal lattice case is termed as +ve charge (–ve charge). Dislocations are composed of pair of disclinations of opposite charge. T_i corresponds to the temperature where disclinations unbind. Thus in the KTHNY mechanism the crystal melts to liquid through two continuous transitions with essential singularities in the thermodynamic quantities and universal jump discontinuities of the dislocation pair interaction strength K and the orientational stiffness K_A, respectively, at the dislocation and the disclination unbinding transitions[36].

---

water ($e \sim 80$), the end surface groups dissociate and provide a large electrostatic negative charge per particle (~ 1000 e for a particle diameter of 1000 Å, where e is the charge of an electron). The counterions (cations like K^+) liberated from the polyballs and additional ions present in the solvent form a cloud around each polyball and hence screen the Coulomb interaction between them. The total interaction potential between two polyballs is generally written as a sum of the short-range London-van der Waal's attraction and the (screened) electrostatic repulsion. Since the attractive part is short-range (~ 20 Å), the particles separated by more than a diameter or so feel only the repulsive part, given by the Derjaguin–Landau–Verwey–Overbeek (DLVO) potential[16,17].

$$V(r) = \frac{(Z^*e)^2}{e}\left(\frac{\exp(kR)}{1+kR}\right)^2 \frac{\exp(-kr)}{r} , \tag{4}$$

where k is the inverse of Debye screening length given by:

$$k^2 = \frac{4p}{ek_B T}[(n_p Z^*)e^2 + \sum_a n_a (z_a e)^2] . \tag{5}$$

Here n_p is the number density of the polyballs of radius R, each having surface charge Z^*e. The additional ions of type a with number density n_a and charge z_a contribute to the screening in addition to the counterions. As can be seen from eqs (4) and (5), the experimental

parameters that can be tuned to control the strength and the range of the inter-particle repulsive interaction are Z_p, e, n_p, n_a. Since for a noninteracting dipolar liquid, e would have behaved inversely as T, the potential and the Boltzmann weight $\exp[-V/k_BT]$ have only a weak temperature dependence. So T is not a good tuning parameter. Furthermore, a change in T could introduce unknown and uncontrolled influx of additional screening charges in the solution due to the activated nature of the ionic dissociation constants of the walls and polyballs themselves. Because of the ease in tuning, usual experiments change the polyball number density n_p and the impurity density n_a to control the interaction potential keeping the temperature fixed all the time. Changing the impurity density n_a effectively changes the range of the interaction. In our simulations we change k to induce a phase transition from crystalline structure to a liquid phase.

The characteristic length and time scales for the colloidal particles are several orders of magnitude larger than those in atomic systems. Micrometer sized colloid particles can be observed in an optical microscope and the large collision times (10s of milliseconds) make real time video of the particles to study the dynamics a possibility. For our purpose the most important property is the high dielectric susceptibility c of the polyballs. The dielectric susceptibility c can be expressed as

$$c = \frac{1}{2} \frac{n_1^2 - n_2^2}{(n_1/n_2)^2 + 2} R^3, \tag{6}$$

where n_1 and n_2 are the refractive indices of the polyballs (~ 1.58) and of the solvent (for water ~ 1.33) respectively; R is radius of polyballs (~ 1000 Å). The typical dielectric susceptibility of polyballs is $c \sim 10^{-13}$ cm^3, which is about a million times larger compared to a conventional atomic system. Dielectric colloidal particles can be manipulated by a laser beam to form extended structures (*Optical matter*[18]). The interaction energy of the colloidal particle in presence of an electric field E is $W = -\frac{1}{2} cE^2$. Interesting effects like the formation of extended structures are possible when the trapping potential W the thermal energy k_BT. Because of the large c this is easily attainable in polyballs as opposed to the atomic systems where such effects would have required prohibitively large external field intensity.

Early experimental studies of two-dimensional melting were on gases such as Ar or N$_2$ adsorbed on solid substrates such as graphite[19] or electron gases confined to 2-d (ref. 20). However, for such studies polyballs offer a number of advantages over the atomic systems. In the latter case the substrate potential from the underlying lattice plays an important role in the melting and specially in the bond-orientational order. In case of the

colloid particles, the substrate can be made absolutely smooth on the length scale of colloidal particles. Charge stabilized colloid particles can be confined to form a monolayer with the typical out of the plane movement less than 1% of the typical in-plane movement. This prevents the problem of vacancies getting created by particles moving out of the plane, which is important since vacancies can have strong effect on the melting transition.

3. Laser-induced freezing

Especially interesting, and the focus of this article, is the physics of a 2-dimensionally confined charge stabilized colloidal system subjected to a one-dimensionally modulated stationary laser intensity pattern (Figure 1). Chowdhury *et al.*[21] obtained such a 2-d system of charge-stabilized colloidal particles by confining them between two glass plates. The glass plates become negatively charged when in contact with the solvent and provide a repulsive force on the negatively charged colloid particles. In response to this repulsion, the polyballs form a monolayer at the center of the experimental cell. For large enough k, the polyball system remains in an isotropic liquid phase. The authors subjected this liquid system to a laser intensity pattern periodically modulated along one direction, which they obtained by superposing two coherent beams at an angle. Using light scattering techniques they found that when the wave-vector of the stationary electric field was tuned to half the wave-vector q_0 where the liquid structure function develops its first peak, a triangular lattice with full two-dimensional symmetry resulted. In the presence of the stationary external field, the system gains energetically by having density modulations corresponding to
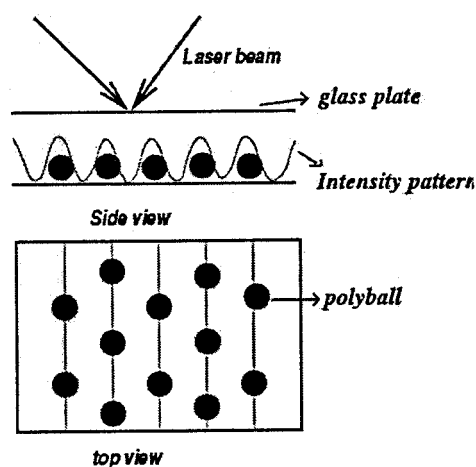

Figure 1. Schematic arrangement of the particles in the intensity pattern due to the external field.

the wave-vector of the modulating field. Because of the nonlinear coupling among the different order parameter modes, beyond a certain external field intensity even the modes which are not directly coupled to the external field become non-zero resulting in a 2d crystal. This phenomenon is christened as laser-induced freezing (LIF).

This apparently simple experiment has nonetheless a rich physics. The 2d nature of the system allows for several scenarios for the melting transition. The external field could also change the nature of transition, in addition to changing the effective transition screening parameter, k. A simple Landau–Alexander–McTague theory, presented by Chowdhury et al.[21] showed a rich phase diagram with a first order transition at the zero external field turning to a second order transition at higher field strengths. At still higher field strengths, the crystalline phase becomes unstable, giving rise to reentrant melting.

The apparently continuous growth of intensities of the crystalline Bragg peaks with increasing external field intensity was taken by Ackerson and Chowdhury[22] as an indication in favour of a second-order transition scenario. Later experimental studies involving direct microscopic observations[23] and simulational studies using the Monte Carlo (MC) technique[24] confirmed the phenomenon of LIF, but without addressing questions connected with the details such as the order of the transition and the phase diagram.

Xu and Baus[25] and Barrat and Xu[26] studied this phenomenon of LIF using density functional theory (DFT)[8]. Their results seemed to indicate that the melting transition remains first order for all values of the external field strength. Chakrabarti et al.[27], in their study of LIF using DFT have shown from general symmetry arguments that, for a suitable choice of the modulation wave-vectors, the free energy expansion for the crystalline phase about the modulated liquid phase (where the density is modulated in one direction in response to the external field, but still the full 2d crystalline structure is missing) contains the relevant order parameters only in even powers. Hence there arises a possibility of change over from the first-order freezing transition at low external field strengths to a continuous transition for large enough external field via a tricritical point[28].

In a later work Chakrabarti et al.[29] studied a two-dimensional colloidal system using Monte Carlo simulation. The use of a standard procedure of looking at finite-size behaviour of the fourth cumulant of the energy[30] seemed to confirm the existence of the tricritical point. Their study also found an intriguing re-entrant modulated liquid phase – where increasing the external field strength actually melted the system instead of taking it towards the crystalline phase.

However, recent, more detailed, simulations by us[9–11] show that the transition remains first order for arbitrarily large field strengths, albeit weakly so. In the presence of the external field, the correlation length near the transition becomes large (though finite) and the entropy difference between the crystalline and the liquid phase becomes small. This hides some of the features of first order character of the transition and one needs to simulate large system sizes to find the true nature of the phase transition. Furthermore, we find that the mechanism for the transition seems to be closely related to the grain boundary induced melting. Our simulation results do not find any re-entrant liquid phase within the statistical uncertainty of the simulation results. These results are discussed in more details in §4 and §5.

Very recently, Wei et al.[31] reported an experimental study of LIF and from the decay of pair correlation function and the real space density plots concluded that their results were in accordance with the results of ref. 29, showing a re-entrant liquid phase. Frey et al.[13] have considered the problem of LIF from the point of view of the dislocation unbinding mechanism and their calculations show that there is a re-entrance in the dislocation unbinding temperature.

4. Monte Carlo simulation and phase-diagram

In this section we discuss in more detail our extensive Monte Carlo simulations of the LIF problem alluded to above. The inter-particle potential is taken to be of DLVO form (eq. (1)) and the external field is modelled as a position dependent potential given by $-V_e\cos(q_0 \cdot x)$, where q_0 is the smallest reciprocal lattice of the triangular lattice [$q_0 \equiv 2p/(\sqrt{(3/2a_0)} (1, 0)$; where a_0 is the lattice spacing]. Besides finite values of V_e, we also have considered the limiting case of infinite V_e, which we simulate by constraining the particles to move only along a set of lines defined by the potential minimum.
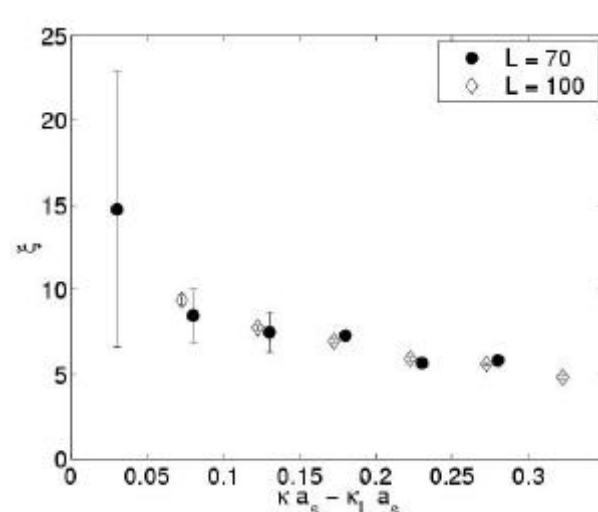

Figure 2. Correlation length for infinite field, as estimated from the decay of the translational order parameter correlation function parallel to external field minima for two different system sizes: 70×70 and 100×100.

In Figure 2 we show the correlation length at $V_e = \infty$, as determined from the decay of the translational order parameter correlations along the y-direction. Near the transition, the correlation length is large but remains finite, signifying a weakly first-order transition. The simulation results obtained for a range of values of V_e and system sizes L fit to a first-order finite-size scaling scenario if the correction terms beyond the leading order are included. The correction terms become more important as one goes to larger values of V_e because the external field greatly reduces the energy and entropy differences between the liquid and the crystalline phase (cf. Table 1).

In Figure 3 we present the phase diagram obtained from the finite-size scaling analysis of the MC simulation data. The computational constraints force us to use system sizes ranging from $L = 8$ to $L = 30$ for finite bV_e and up to $L = 100$ for $bV_e = \infty$ (where motion in one direction is frozen leading to less computational requirement for a particular system size as compared to finite bV_e). Still the L values (even for $bV_e = \infty$) are small enough that we had to use correction terms to usual leading order finite-size scaling relations to estimate the infinite system quantities[9]. Our extensive

Table 1. Results from finite-size scaling of the Monte Carlo data

bV_e	$k_\infty * a_s$	$b(E_+ - E_-)$
0.0	14.34 ± 0.02	0.071 ± 0.0067
2.0	15.66 ± 0.03	0.0044 ± 0.0031
∞	15.62 ± 0.05	0.0014 ± 0.0004

Figure 3. Phase diagram of laser-induced freezing, obtained from finite size scaling.

simulations do not show any re-entrant transition to the modulated liquid phase at high fields, as opposed to earlier simulation results[29]. The scaling analysis also gives the jump in internal energy at the transition (Table 1). For large bV_e, the system sizes used in ref. 29 were much smaller than those presented here and comparable to the correlation length. Hence, for large external fields they were below the range of system sizes where the finite-size scaling analysis is valid. This could have led to apparent signatures of a second-order transition in ref. 29. In a first order scenario, the height of the specific heat peak is proportional to the square of the internal energy difference between the two phases at the phase transition. Thus the peak height of the specific heat becomes small with increasing field strength. The averaging done in ref. 29 was not enough to resolve this small peak from the statistical noise. With similar averaging as of ref. 29, we also find from our simulation data that spurious peaks appear in the specific heat data. The base line of the specific heat increases with decreasing k. This probably led to a biased search for specific heat peaks at low values of k and a spurious peak was probably mistakenly identified as a true specific heat peak, leading to the phase diagram with re-entrant melting in ref. 29.

Our MC results and mean-field analysis show that the modulated liquid phase is liquid crystalline in nature with nonzero anisotropic shear rigidity. The external field couples to the bond-orientational order parameter also. So even for parameters where in absence of the external field the system freezes through a two-stage continuous transition (KTHNY mechanism), the disclination unbinding transition will be wiped out in the presence of a finite bV_e (ref. 10).
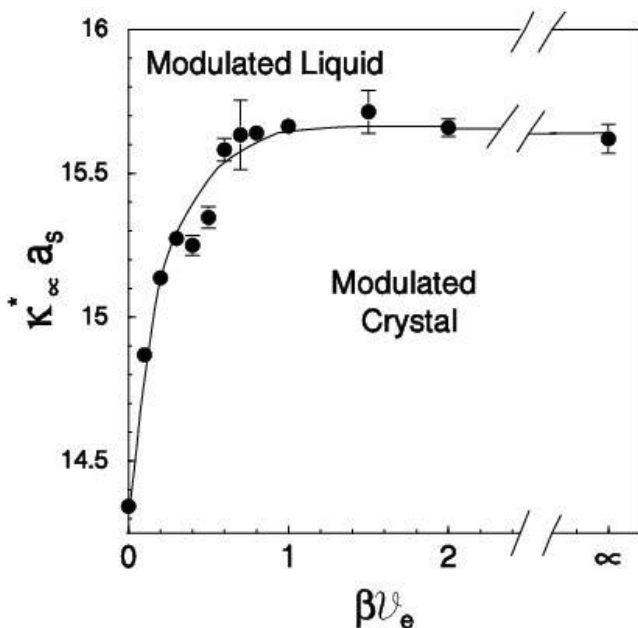
5. Dynamics of melting: Grain-boundaries and slide-boundaries

Simulation of 2-d systems offers the possibility of visualizing the defect structures that arise in the simulated configurations. Since the melting transition in 2-d is known to be dominated by the topological defects, such visualization can aid in distinguishing among the different scenarios that have been proposed for the 2-d melting. Also, because one is interested in the dynamics of the melting mechanism, one does not need the large equilibration time needed for simulating large systems sizes. Hence we have studied the same system as discussed above using a Brownian dynamics simulation.

In the configurations generated in the simulation, disclinations are identified by constructing the Voronoi cell for each of the particles. At any finite temperature, the particles move around about the lattice points. Moving a single particle by a small amount can generate a dislocation pair or a small cluster of disclinations with

net Burgers vector being zero and which do not have any energy barrier against annihilation. Many such clusters can form and disappear without facing any energy barrier. At finite temperatures, it is therefore to be expected that subsequent configurations will have some new defect structures while some of the older ones disappear. These 'virtual defects' present in any given configuration can be removed by moving the system 'downhill' in energy. The resulting configuration is called 'inherent structure'. The construction of the inherent structure does not change any of the qualitative features of the actual configuration generated in the simulation, but helps one to identify the long lived defects contained in them in a clean way.

From our Brownian dynamics simulations[10], in absence of the external field, we find that as k is increased, the number of dislocation pairs increase, they form small loops, the loops merge with each other and eventually result in forming grain boundaries that cover the full system at the melting transition – so that both the translational and the orientational orders disappear simultaneously.

In Figure 4, we have shown the inherent structure corresponding to $ka_s = 14.5$ at zero field, where the crystal
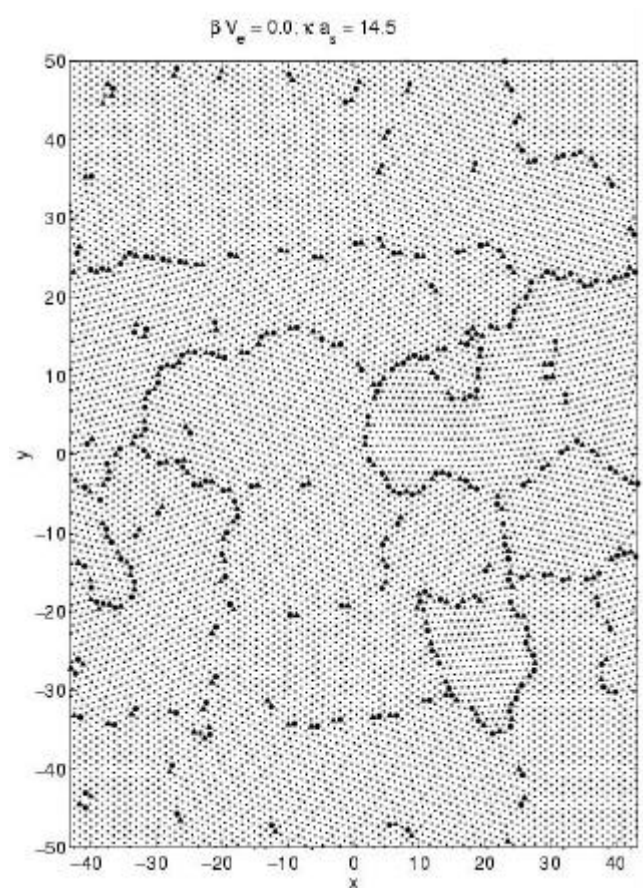

Figure 4. Grain boundaries in the inherent structure for a typical zero field liquid configuration. The triangles, circles and stars correspond to $z = 5, 7$ and 8 respectively.

has melted. The inherent structure has a number of micro-crystallites whose orientations change abruptly as one crosses the grain-boundaries separating them. The grain-boundaries are formed by oriented strings of dislocations[32].

In the presence of the external modulating potential, the bond-orientational order remain long-ranged[10]. So, the usual grain-boundaries with non-zero Burgers vectors (which would imply that the orientation of the crystallites changes as one crosses the grain-boundary) are energetically unfavourable. In the liquid configuration in presence of finite field, we find that a large number of correlated defects are present. Here the orientation is same throughout the sample and the correlated defects which define different patches are essentially small collections of dislocations which have net zero Burgers vector.

In order to analyse the finite bV_e defect structures in more detail, we define a local order parameter at the position of particle m as, $r_d^m \equiv \exp[i\vec{G}_d \cdot \vec{r}_m]$, with G_d being one of

$$\left[\frac{2p}{\sqrt{3}/2}\left(\pm\frac{1}{2}, \pm\frac{\sqrt{3}}{2}\right)\right],$$

which together with $\pm q_0 \hat{x}$, define the first shell of the crystalline reciprocal lattice vectors (rlv). Neighbouring particles m and n, which satisfy the condition $|r_d^m + r_d^n| \geq 1.8$, are considered to be in the same cluster (for a perfect lattice, the value would have been 2, while for completely uncorrelated particles, the value of the sum would be 0). After identifying such clusters, each cluster is assigned the mean value of the phase of r_d^n for n being a member of the cluster. We have checked that variations in this coarse graining procedure do not lead to qualitatively different results.

Figure 5 shows the phase of $r_d(r)$ constructed in this way, superposed with the 'inherent' defect structure for $bV_e = 5.0$ and $ka_s = 15.4$, which corresponds to the crystalline phase. The small number of defects present locally create regions with phase mismatch. But by and large the phase remains same over the full system and averaging over the configuration gives non-zero value of the order parameter. In contrast, in Figure 6, corresponding to $ka_s = 16.0$, where the system is in the modulated liquid phase there is a proliferation of defects, which succeed in breaking up the system into parts with completely uncorrelated phases of the order parameter. The 'grains' now have a fixed orientation, and the corresponding 'grain-boundaries' are 'slide-boundaries'.
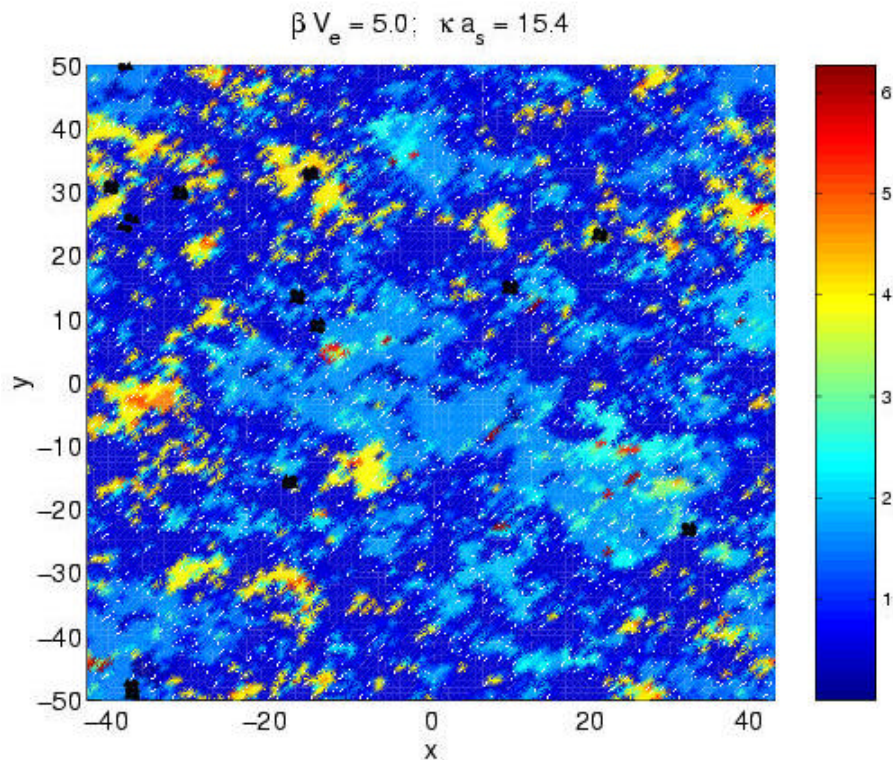
Figure 5. Phase of order parameter r_d in the crystal. The triangles, circles and stars respectively denote particles with coordination number 5, 7 and 8, i.e. correspond to disclinations. The defect structures induce local phase mismatches. But still there is long-range phase correlation leading to a non-zero order parameter value, as the defects are tightly bound.
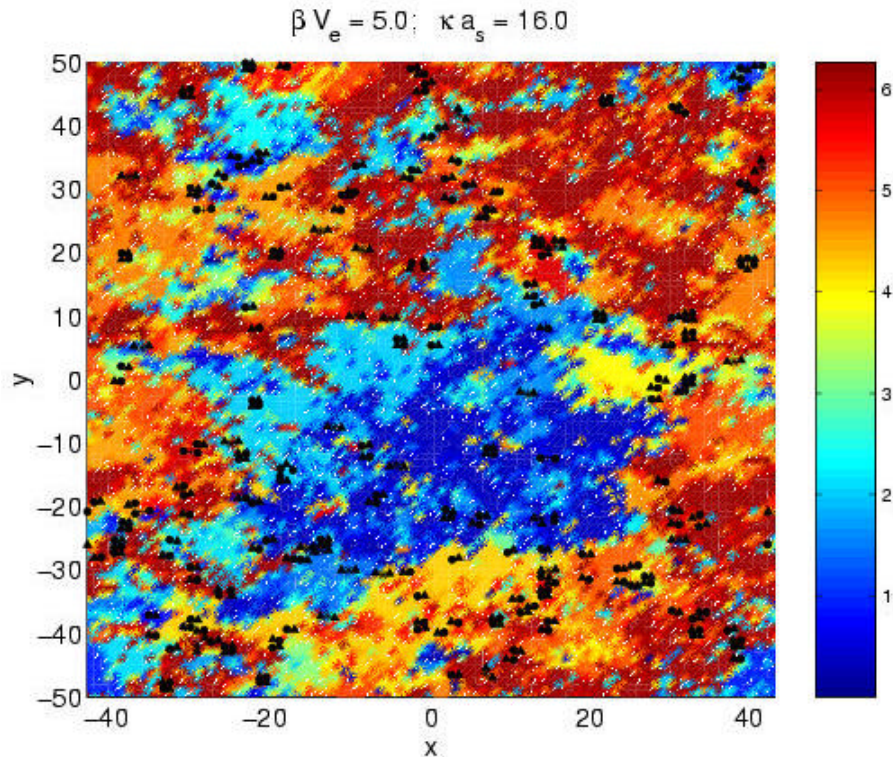

Figure 6. Phase of order parameter r_d in the liquid. The triangles, circles and stars respectively denote particles with coordination number 5, 7 and 8, i.e. correspond to disclinations. Correlated defect structures break up the system in grains which does not match in the order parameter phase. The order parameter becomes zero, when averaged over the full system.

6. Laser-induced freezing in hard-sphere colloids

In the limit of very high screening, i.e. large k, charge stabilized colloids can be well approximated as a hard-sphere system, i.e. with a model potential between the particles given by: $V(r) = \infty$ $(r < R)$, $0 (r > R)$. There are other systems such as sterically stabilized colloids which are also good candidates for being described by this model. Hence, it is of obvious interest to study LIF in such a model system.

We have recently carried out Monte Carlo simulation of LIF in a 2-d hard sphere, i.e. hard-disc system. The relevant control parameter is the area fraction (f). In our simulations, we change the area fraction by changing the diameter of the particles, while the box size and the number of particles (900) are held fixed. Temperature is not a relevant quantity for this system when the external potential is absent; but in the presence of the potential, we choose the unit of energy chosen as the thermal energy $k_B T$. The typical number of configurations which have been simulated in order to compute the equilibrium averages is of the order of 5×10^6.

The translational order parameter for the kth rlv, $\vec{\mathbf{q}}_k$ is calculated as

$$r_{\vec{\mathbf{q}}_k} = \left\langle \frac{1}{N} \left| \sum_i \exp(i\vec{\mathbf{q}}_k \cdot \vec{\mathbf{r}}_i) \right| \right\rangle. \tag{7}$$

This definition removes any dependence on the origin of co-ordinates. The order parameter so defined is of order unity in the crystalline state, while in the liquid state it goes to zero as $1/N^{1/2}$ for a system of N particles.

We denote by r_l the order parameters for the wave-vectors parallel to the modulation wave-vector, e.g.

$$\vec{\mathbf{q}}_1 = \frac{2p}{a\sqrt{3}/2}(1, 0),$$

and by r_d the order parameters for the other four first-shell wave-vectors, such as

$$\vec{\mathbf{q}}_2 = \frac{2p}{a\sqrt{3}/2}\left(\frac{1}{2}, \frac{\sqrt{3}}{2}\right).$$

In Figure 7 a we have plotted r_d for the cases when there is no external field and when the field strength is infinite. In the case of zero field, entropy is the only mechanism that is forcing the density modes at the wave vectors $\vec{\mathbf{q}}_k$ to develop, and this happens at a packing fraction of about 0.7. For the case of infinite strength, the external potential is so large that the freedom of the particles to move in the x-direction is totally suppressed and hence they can execute motion only in the y-direction. Now we find that r_d becomes sizeable when the area fraction exceeds 0.68. This value of the area-fraction corresponds to the situation when there is vertical contact between the particles for the first time. For all area fractions less than 0.69, the system consists of L uncoupled 1-dimensional chains of particles, with particles in the same line interacting through the hard-sphere repulsive potential. We know that a disorder-to-order transition is not possible in a 1-dimensional system with short-ranged interactions. Hence there is no ordering before $f = 0.69$. Development of the density mode corresponding to the wave-vector $\mathbf{q}_2$ occurs only when a coupling between two neighbouring chains is established through vertical contact. To identify the threshold for the transition from the modulated liquid to modulated crystal phase, we have plotted dr_d/df as a function of f in Figure 7 b. It can be seen
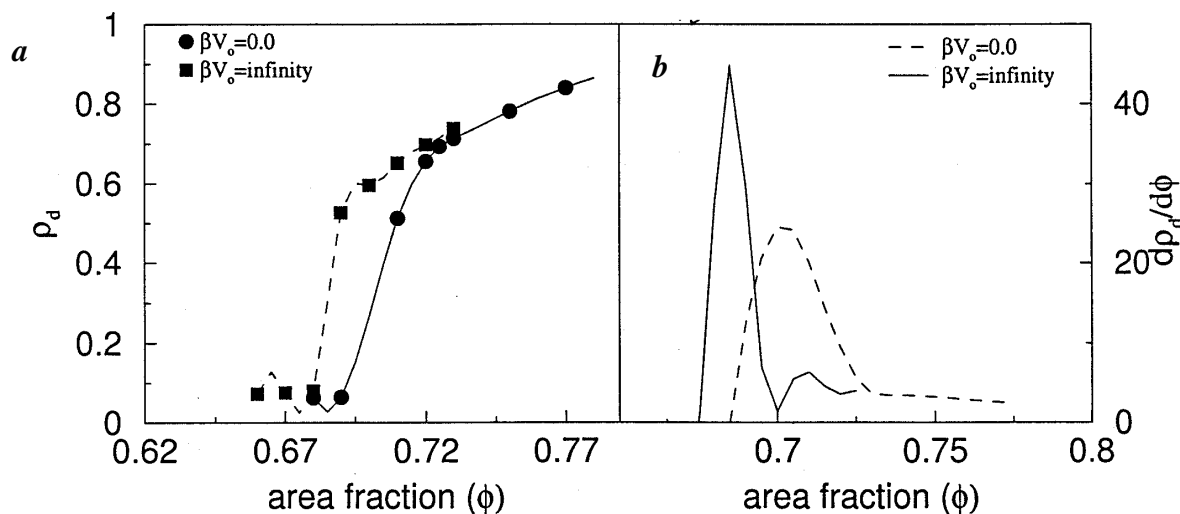

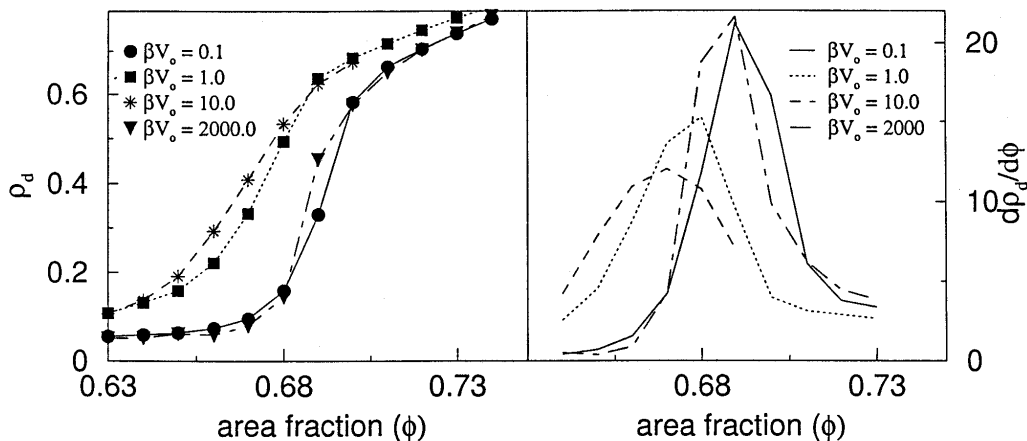**Figure 7.** Variation of r_d (a) and dr_d/df (b) for $bV_0 = 0$ and for infinite field.

Figure 8. Plots of r_d and dr_d/df for some typical values of field strength, $bV_0 = 0.1$, 1.0, 10.0 and 2000.

that dr_d/df has a pronounced peak at certain f signifying sharp change in r_d at that value of f. We identify the peak in dr_d/df as the onset of the freezing transition leading to a non-zero density mode r_d. These area fractions for the zero-field and infinite-field are 0.702 and 0.688, respectively.

In Figure 8, we have plotted the variation of r_d and dr_d/df with changing area fractions for some typical values of field strength ($bV_0 = 0.1$, 1.0, 10.0, 2000.0, where $b = 1/k_BT$). From the plots we have identified, for each value of bV_0, the corresponding value of f where the onset of freezing occurs. Using these values, we have thus constructed the phase diagram of the hard-sphere colloidal system in the presence of an external laser field, which is plotted in Figure 9.

As noted above, in the absence of the laser field, the onset of freezing takes place at an area fraction value of 0.702. When the field is switched on, the density modes (r_1) corresponding to the modulating wave-vector become nonzero, and this facilitates the development of the other density modes (r_d) causing the freezing transition to happen at a smaller f. As we can see from the phase diagram, the value of f required for freezing continues to decrease till a bV_0 value of 2.0, where it is down to 0.667. Then it increases again to reach the infinite-field limit of about 0.69. A possible explanation for this latter increase could be the following. As bV_0 gets increased to values much larger than unity, the motion of the particles become more and more restricted to be around the lines $q_0 x = (2n + 1)p$. Thus, beyond a threshold value of the field strength, the influence of particles of neighbouring lines on the motion of particles on a particular line decreases. This manifests in the fact that the condensation of the density mode r_d takes place at a higher area fraction compared to the values corresponding to field strengths below that threshold. With increasing field strength, the value of the critical f goes on increasing until it reaches the limiting value of 0.688.
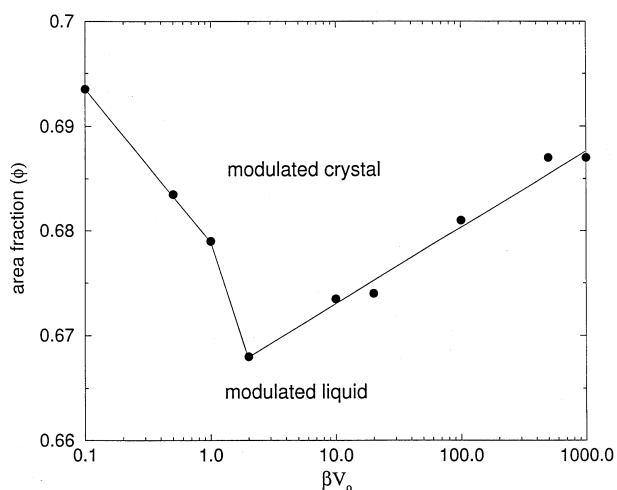

Figure 9. Phase diagram of the colloidal system for 900 particles in an external laser field.

If we examine the phase diagram in Figure 9, we can see that for any fixed value of f less than 0.66, the colloidal system continues to be in modulated liquid state for all values of bV_0. For values larger than 0.7, the system remains in crystalline form throughout the entire range of field strengths. The intermediate region is interesting. For example, consider a f value of 0.675. For low field strength, at this volume fraction, the system behaves like a modulated liquid. If one exceeds a certain field strength ($bV_0 = 1.4$), the system undergoes a transition to a modulated crystalline state. But beyond $bV_0 = 31$, the hard sphere system again becomes a modulated liquid. Thus, from the measurement of the translational order parameter in Monte Carlo simulations, we find a possibility of re-entrant behaviour in the two-dimensional hard sphere system in the presence of an external modulation potential.

To examine the three phases at $f = 0.675$, we have measured in our simulations the equilibrium real-space particle density $\langle r(x, y) \rangle$ for three different field strengths, by averaging over 1.5×10^5 configurations
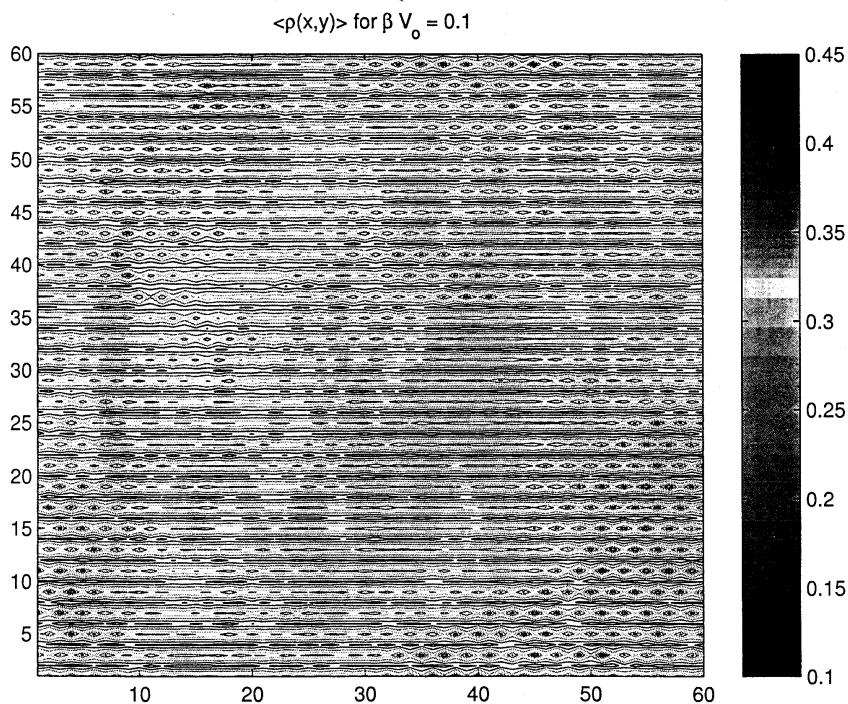
$<\rho(x,y)>$ for $\beta\,V_0 = 0.1$

Figure 10. Contour plot of the average density for $f = 0.675$ in the presence of a modulation potential with $bV_0 = 0.1$ corresponding to the modulated liquid phase.
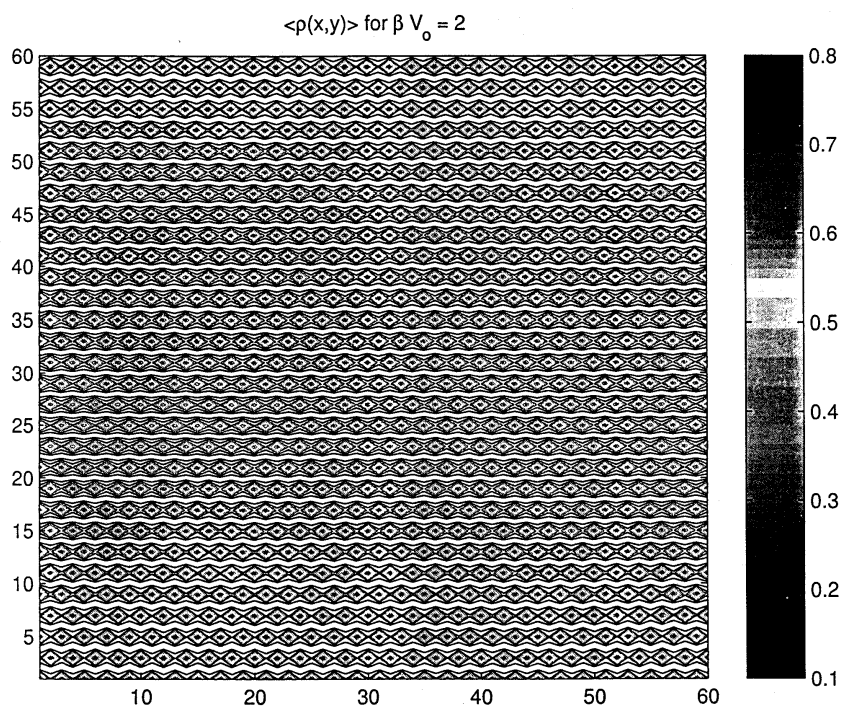
$<\rho(x,y)>$ for $\beta\,V_0 = 2$

Figure 11. Contour plot of the average density for $f = 0.675$ in the presence of a modulation potential with $bV_0 = 2.0$ corresponding to the crystalline phase.

after equilibrating for 10^5 configurations. The results are shown in Figures 10–12.

From the plots, we can see that for bV_0 is equal to 0.1, the system is in a liquid state, the modulations not being very prominent. When bV_0 is equal to 2.0, the system is nearly crystalline and for $bV_0 = 1000$, the system loses its crystalline structure and again becomes a modulated liquid. This confirms the occurrence of a re-entrant melting as a function of the strength of the modulating potential. This is consistent with the recent prediction
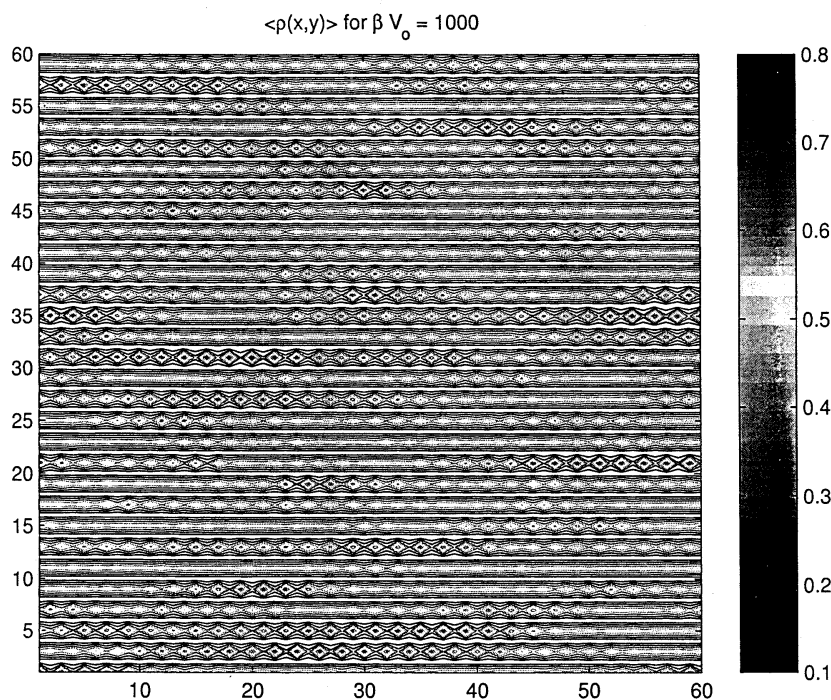
$<\rho(x,y)>$ for $\beta V_0 = 1000$

Figure 12. Contour plot of the average density for $f = 0.675$ in the presence of a modulation potential with $bV_0 = 1000.0$ corresponding to the reentrant liquid phase.

by Frey *et al.*[13], but it remains to be shown that the melting here is a continuous transition and is mediated by the unbinding of dislocations. More extensive simulations are needed to demonstrate the latter. Meanwhile, it would be interesting to carry out experiments involving hard sphere colloidal particles and observe whether such a reentrant melting occurs as the strength of the laser field is increased.

After the above work was completed, we learnt of an independent and more extensive Monte Carlo simulational study on the same system by Strepp *et al.*[33]. Their phase diagram, obtained using the cumulant intersection method, is qualitatively and quantitatively similar to the one obtained by us. This further strengthens the case for the existence of the re-entrant modulated liquid phase in a hard-sphere colloidal system subject to an external laser field modulation.

7. Remarks

In this review we have presented our recent simulation results on laser-induced freezing in charge stabilized colloids which show that for the system considered, the transition is weakly first order for all values of the applied field. In the absence of the external field, the crystal seems to melt via the generation of grain-boundaries. At finite fields, slide-boundaries would seem to be responsible for destroying the order.

It is generally accepted that at high core energies, the melting transition in 2-d follow the dislocation unbinding route (KTHNY) and there is a hexatic phase between the crystalline and the liquid phases. Armstrong *et al.*[5] in their experiments find that the transition is either through dislocation unbinding or generation of grain-boundaries depending on the polyball diameter. The particle diameter in our simulations correspond to the value where Armstrong *et al.*[5] find generation of grain-boundaries. It will be interesting to do simulations at different particle sizes and test the predictions of Frey *et al.*[13] on dislocation unbinding picture of LIF, as well as understand the crossover from that mechanism to the grain/slide-boundary mechanism for LIF.

1. Kosterlitz, J. M. and Thouless, D. J., *J. Phys. C*, 1973, **6**, 1181.
2. Halperin, B. I. and Nelson, D. R., *Phys. Rev. Lett.*, 1978, **41**, 121.
3. Young, A. P., *Phys. Rev. B*, 1979, **19**, 1855.
4. Chui, S. T., *Phys. Rev. Lett.*, 1982, **48**, 933.
5. Armstrong, A. J., Mockler, R. C. and OSullivan, W. J., *J. Phys. Cond. Matter*, 1989, **1**, 1707.
6. Saito, Y., *Phys. Rev. Lett.*, 1982, **48**, 1114.
7. Strandburg, Katherine, J., *Phys. Rev. B*, 1986, 3536.
8. Ramakrishnan, T. V. and Yussouf, M., *Phys. Rev. B*, 1979, **19**, 2775.
9. Das, C., Sood, A. K. and Krishnamurthy, H. R., cond-mat/9902006.
10. Das, C., Sood, A. K. and Krishnamurthy, H. R., *Phys. A*, 1999, **270**, 237.
11. Das, C., Sood, A. K. and Krishnamurthy, H. R. (submitted to *Europhys. Lett.*), 1999.

12. Chaudhuri, Pinaki, Sood, A. K. and Krishnamurthy, H. R. (unpublished), 2000.
13. Frey, E., Nelson, D. R. and Radzihovsky, L., *Phys. Rev. Lett.*, 1999, **83**, 2977.
14. Pieranski, Pawel, *Contemp. Phys.*, 1983, **24**, 25.
15. Sood, A. K., in *Solid State Physics* (eds Ehrenreich, H. and Turnbull, D.), Academic Press, New York, 1991, vol. 45, pp. 1–73.
16. Derjaguin, B. V. and Landau, L. D., *Acta Phys. Chim.*, *USSR*, 1941, **14**, 633.
17. Verwey, E. J. W. and Overbeek, J. Th., *Theory of Stability of Lyophobic Colloids*, Elsevier, Netherlands, 1948.
18. Burns, M. M., Fournier, J. M. and Golovchenko, J. A., *Science*, 1990, **249**, 749.
19. Dash, J. G., *Films on Solid Surfaces*, Academic Press, New York, 1975.
20. Cole, M. W., *Rev. Mod. Phys.*, 1974, **46**, 451.
21. Chowdhury, A., Ackerson, B. and Clark, N. A., *Phys. Rev. Lett.*, 1985, **55**, 833.
22. Ackerson, B. J. and Chowdhury, A., *Faraday Discuss. Chem. Soc.*, 1987, **83**, 309.
23. Loudiyi, K. and Ackerson, B. J., *Phys. A*, 1992, **184**, 1.
24. Loudiyi, K. and Ackerson, B. J., *Phys. A*, 1992, **184**, 26.
25. Xu, H. and Baus, M., *Phys. Lett. A*, 1986, **117**, 127.
26. Barrat, J. L. and Xu, H., *J. Phys. Cond. Matter*, 1990, **2**, 9445.
27. Chakrabarti, J., Krishnamurthy, H. R. and Sood, A. K., *Phys. Rev. Lett.*, 1994, **73**, 2923.
28. Unlike the predictions of the DFT calculations in ref. 27, our simulation results indicate a first order transition for all values of bV_e. The simple density functional theory of ref. 27 uses $c^{(2)}$ of the isotropic liquid as input. It is known that such DFT calculation is quantitatively wrong (for example, the structure factor peak height is off by a factor of around 30%). One possibility is that the higher order correlations change the relative signs of the effective coefficients in the Landau free energy expansion about modulated liquid phase – leading to a first order transition, as opposed to the prediction of simple DFT of ref. 27. The other possibility is that the first-order transition seen in our simulations is driven by fluctuations not present in DFT calculation, which is a mean field theory.
29. Chakrabarti, J., Krishnamurthy, H. R., Sengupta, S. and Sood, A. K., *Phys. Rev. Lett.*, 1995, **75**, 2232.
30. Challa, Murthy, S. S., Landau, D. P. and Binder, K., *Phys. Rev. B*, 1986, **34**, 1841.
31. Wei, Q. H., Bechinger, C., Rudhardt, D. and Leiderer, P., *Phys. Rev. Lett.*, 1998, **81**, 2606.
32. Burgers, J. M., *Proc. Phys. Soc.*, 1940, **52**, 23.
33. Strepp, W., Sengupta, S. and Nielaba, P., preprint (cond-mat/0010345).
34. Murray, C. A., in *Bond-Orientational Order in Condensed Matter Systems* (ed. Strandburg, K. J.), Springer, New York, 1992.
35. Nabarro, F. R. N., *Theory of Crystal Dislocations*, Clarendon, Oxford, 1967.
36. Nelson, D. R., in *Phase Transitions and Critical Phenomena*, (eds Domb, C. and Green, M. S.), Academic Press, London, 1983, vol. 7, p. 1.